applied sciences

MDPI

Article

A Fracture Mode-Constrained Physics-Informed Machine Learning Framework for Predicting Acoustic Emission Energy of Coal Gangue Backfill

Jiahui Li [1], Pengfei Wu [2,*], Jiaxu Jin [2], Bing Liang [1], Zhiqiang Lv [2] and Shenghao Zuo [3]

[1] School of Mechanics and Engineering, Liaoning Technical University, 47 Zhonghua Road, Fuxin 123000, China
[2] School of Civil Engineering, Liaoning Technical University, 47 Zhonghua Road, Fuxin 123000, China
[3] School of Water Conservancy and Transportation, Zhengzhou University, Zhengzhou 450001, China
* Correspondence: wpf_605@163.com

Abstract

Coal gangue backfill serves as a primary supporting structure for overlying strata in mined-out areas, and its internal damage evolution is directly associated with the safety and stability of mining operations. Acoustic emission (AE) technology provides an effective approach for investigating damage evolution by capturing transient strain energy release events within materials in real time. However, conventional AE analysis methods predominantly rely on statistical interpretations of individual parameters, making them insufficient for revealing the underlying physical mechanisms governing the influence of fracture characteristics on energy evolution pathways. To address the aforementioned limitations, this paper proposes a fracture mode-informed physics-enhanced machine learning framework for predicting acoustic emission energy evolution in coal gangue backfill. First, based on the AE monitoring data of coal gangue backfill under uniaxial compression (a total of 18,992 valid AE events from three parallel specimens with identical mix proportion), the RA–AF parameters combined with the K-means unsupervised clustering algorithm were employed to automatically identify tensile and shear fracture modes, thereby constructing physically meaningful fracture mode labels. Second, the fracture mode information was integrated with AE statistical features, including rise time, duration, amplitude, counts, peak frequency, and center frequency. After selecting the most informative features using the minimum-redundancy, maximum-relevance (mRMR) algorithm, a Bayesian optimization-based support vector regression (BO-SVR) model was developed for AE energy prediction. The results demonstrated that after incorporating the fracture mode-based physical labels, the proposed model achieved a coefficient of determination (R^2) of 0.9027 on the testing dataset, with an RMSE of 0.1562 and an MAE of 0.1204. Ablation experiments further confirmed that the introduction of fracture mode labels improved the R^2 value by approximately 3.4% compared with the model without physical constraints. Fivefold cross-validation yielded an average R^2 of 0.9460 with a standard deviation of 0.0023 for the SVR model. Furthermore, per-specimen independent holdout validation yielded an average R^2 of 0.9044 with a standard deviation of 0.0512 across three independent specimens, confirming the excellent stability and repeatability of the proposed framework. The original single-specimen results (4083 events, R^2 = 0.9727) are provided as a baseline reference. Mechanistic analysis revealed that the average energy release associated with shear fractures was approximately 739 times that of tensile fractures, demonstrating that fracture mode information provides physically consistent mechanical constraints for the machine learning model. This study provides an effective new method for the stability evaluation and intelligent monitoring of coal gangue filling materials.

Check for updates

Received: 10 September 2026
Revised: 25 September 2026
Accepted: 28 September 2026
Published: 30 September 2026

Copyright: © 2026 by the authors. Licensee MDPI, Basel, Switzerland. This article is an open access article distributed under the terms and conditions of the Creative Commons Attribution (CC BY) license.

Keywords: coal gangue backfill; acoustic emission; physics-informed enhancement; fracture mode identification; energy prediction

1. Introduction

The large-scale accumulation of coal-based solid waste in coal-mining areas poses potential threats to the surrounding ecological environment. With the rapid development of green mining technologies and the coordinated utilization of solid waste in China, coal gangue backfill mining has become an important approach to mitigating surface subsidence and addressing the challenges associated with solid-waste disposal [1–3]. As a major load-bearing structure within the overburden above mined-out areas, coal gangue backfill plays a critical role in maintaining the stability of underground mining systems, and its internal damage evolution is directly related to mine safety and production [4,5]. Accurate estimation of AE energy is critical for real-time damage assessment and early warning of backfill instability in engineering monitoring. However, field AE energy calculation is susceptible to noise and system calibration deviations, while conventional waveform parameters can be obtained stably in real time. Accordingly, extensive research has been conducted worldwide on the damage evolution behavior of rock-like materials.

Continuum damage constitutive models can describe the macroscopic degradation of material strength, but they generally neglect the discontinuous behavior arising from internal structural heterogeneity [6–8]. To address this limitation, statistical strength theories, such as the Weibull distribution, have been introduced to characterize the stochastic behavior of microscopic elements under loading. For example, Shi et al. [9] employed a Weibull distribution model to investigate the freeze–thaw degradation behavior of geopolymer mortar and predict its service life. Deng et al. [10] combined a Weibull function with a Kalman filter to develop a predictive model, in which the Weibull function captured long-term deformation trends while the Kalman filter dynamically assimilated time-series InSAR observations to identify the actual fluctuations in surface uplift in closed coal-mining areas. However, these approaches rely primarily on empirical fitting at the macroscopic scale and are therefore limited in their ability to reveal the underlying physical relationships between fracture characteristics and energy evolution pathways.

Acoustic emission (AE) technology provides an effective means of investigating damage evolution in quasi-brittle materials by capturing transient strain-energy release events generated within materials in real time [11,12]. For example, Wu et al. [13] prepared gypsum-based rock-like specimens containing fractures with different inclination angles and numbers and conducted uniaxial compression tests. By combining AE monitoring with digital image correlation (DIC), they investigated the effects of fracture characteristics on the mechanical behavior and failure evolution of rock-like materials. Tian et al. [14] conducted AE tests under uniaxial compression to investigate the effects of initial stress conditions and reloading intervals on the stress-memory capacity of granite, i.e., the Kaiser effect. RA–AF-based fracture mode classification is a widely accepted methodology in AE quantitative analysis, and has been further validated by recent studies combining wave propagation analysis [15]. However, conventional AE analysis largely relies on statistical interpretation of individual parameters, making it difficult to accurately identify fracture modes and elucidate their underlying mechanisms. To enhance the intelligence of AE-based damage identification, Zhou et al. [16] developed a deep learning model incorporating a self-attention mechanism to capture elastic-wave signals generated during damage evolution, enabling the intelligent identification of damage modes in carbon fiber-reinforced polymer (CFRP) tubes with different dimensions and overcoming the limited adaptability

of conventional identification models to variations in specimen size. Kwon et al. [17] proposed a data-driven AE framework with multimodal validation for characterizing mesomechanical damage in particle-reinforced composites. By integrating microscopic and diffraction-based techniques, they demonstrated that a sharp increase in AE activity within specific frequency bands associated with particle damage can serve as a precursor to the accelerated accumulation of internal damage. These studies demonstrate the substantial potential of intelligent and multimodal AE analysis. Nevertheless, for cemented backfill materials, physically based characterization of fracture modes and their relationship with energy release remain insufficiently investigated.

In recent years, with the rapid development of machine learning in the field of geotechnical engineering [18–21], data-driven models have demonstrated considerable potential for AE signal analysis and mechanical property prediction. Physics-informed machine learning, which integrates physical prior knowledge into data-driven models, has become an important paradigm to improve model interpretability and generalization [22]. For example, Lü et al. [23] employed two ensemble algorithms, namely Bayesian optimization-enhanced random forest (RF) and extreme gradient boosting (XGBoost), together with three non-ensemble algorithms, namely support vector regression (SVR), decision tree (DT), and multilayer perceptron (MLP), to train and predict consolidation yield stress using both the raw and preprocessed datasets, and comparatively evaluated the predictive performance of these models for the yield stress of geotechnical materials. Lu et al. [24] proposed a crow search algorithm (CSA)-optimized backpropagation neural network (CSA-BP) model for the inversion of mechanical parameters of post-earthquake slopes and combined it with the discrete element method to evaluate the stability of hazardous rock slopes under aftershock loading. However, purely data-driven approaches generally suffer from limited physical interpretability and are susceptible to interference from high-dimensional redundant features, which can consequently compromise the generalization capability and reliability of predictive models [25,26]. Meysami et al. [27] further demonstrated that proper physical constraints and regularization can effectively improve model stability and generalization performance on small-scale engineering datasets.

Based on the above considerations, this paper proposes a machine learning framework that integrates fracture-mode physical information to predict the evolution of acoustic emission (AE) energy in coal gangue backfill. In this context, “physics-informed” refers to incorporating explicit mesoscopic fracture mechanism knowledge as prior constraints into the model, rather than embedding governing differential equations. The fracture mode identified by classical AE criteria is transformed into a physically meaningful state variable to guide model optimization. Fracture modes are identified using the RA–AF parameters and subsequently transformed into physics-informed priors with explicit mechanical significance. These are integrated with AE statistical features and jointly used as inputs to a Bayesian optimization-based support vector regression (BO-SVR) model, enabling fracture mechanism-aware prediction of AE energy evolution. The main contributions of this study are as follows.

(1) A fracture mode-aware physics-informed feature construction method was proposed, in which the fracture-mode identification results obtained from RA–AF analysis were explicitly transformed into physics-informed prior variables and integrated with AE statistical features, enabling the machine learning model to account for fracture formation mechanisms rather than relying solely on statistical responses of AE signals.
(2) The contribution of fracture-mode physical information to AE energy prediction was quantitatively elucidated. Through ablation experiments and feature-importance analysis, the results demonstrated that fracture-mode information can effectively

complement conventional AE features, thereby improving both prediction accuracy and the generalization stability of the model.

(3) The physical relationship between fracture-mode evolution and AE energy release was established, revealing the transition in energy-release mechanisms as coal gangue backfill evolves from tensile-dominated fracturing to shear-dominated failure. This finding provides a mechanical basis for fracture mechanism-aware intelligent damage monitoring.

2. Data Acquisition and Feature Engineering

2.1. Experimental Data Description

The acoustic emission (AE) data used in this study were obtained from uniaxial compression tests of coal gangue-filled backfill (CGFB) specimens. The specimens were prepared using ordinary Portland cement, fly ash, iron tailings, and coal gangue. The detailed preparation procedures and experimental scheme followed the methodology reported in our previous study [28]. All specimens were cured under standard curing conditions (temperature: 20 ± 2 °C; relative humidity: approximately 98%) for 28 days before mechanical loading tests were conducted.

The uniaxial compression tests were conducted using a servo-controlled loading system, while AE signals were simultaneously recorded during the loading process. The AE monitoring system consisted of a DS5 AE acquisition unit equipped with RS-2A AE sensors. The sensors were symmetrically arranged on the specimen surface, and petroleum jelly was applied as a coupling agent to ensure effective transmission of AE signals. The AE acquisition parameters were set as follows: a sampling frequency of 3 MHz, a pre-amplifier gain of 40 dB, and a threshold amplitude of 45 dB.

A total of 18,992 valid AE events were obtained from three standard cylindrical CGFB specimens with identical mix proportion and curing conditions. The three specimens contain 6939, 6317, and 5736 valid events, respectively. The extracted AE parameters comprised rise time, duration, amplitude, energy, counts, peak frequency, and center frequency. Based on these AE parameters, the RA and AF values were further calculated for fracture mode identification. All specimens were tested under the same loading protocol and AE acquisition parameters to ensure data consistency. Subsequently, the identified fracture mode information was introduced into the machine learning framework as physics-informed prior knowledge to achieve AE energy prediction.

2.2. Fracture Mode Identification Based on RA–AF Features and Physics-Informed Feature Construction

Acoustic emission (AE) signals not only reflect the internal crack activity of materials but also contain critical information regarding fracture mode evolution [29–31]. During the compression-induced failure process of coal gangue backfill, crack propagation generally occurs through two dominant mechanisms: tensile fracture and shear sliding. Different fracture modes correspond to distinct energy release mechanisms [32–35]. Therefore, incorporating fracture evolution information into machine learning models can enhance the physical interpretability of prediction results.

In this study, the RA–AF analysis method was employed to identify fracture modes of AE events. The RA value was defined as the ratio of rise time to peak amplitude, whereas the AF value was defined as the ratio of counts to duration.

According to the acoustic emission-based fracture identification theory, tensile fractures generally exhibit rapid energy release characteristics, with shorter rise times and higher amplitudes, resulting in lower RA values and higher AF values. In contrast, shear fractures involve frictional sliding along crack surfaces, leading to longer fracture processes

and consequently higher RA values and lower AF values. Therefore, the distribution characteristics in the RA–AF parameter space can effectively characterize the differences between distinct fracture modes.

To eliminate the subjectivity associated with manually defined fracture classification boundaries, an unsupervised clustering strategy was adopted to automatically identify fracture modes within the RA–AF feature space. Before clustering, RA and AF features were normalized by Z-score (zero mean, unit variance) to eliminate the influence of magnitude difference between the two parameters. The RA and AF features extracted from all AE events were used as input variables for the K-means clustering algorithm, which partitions AE events into different clusters by minimizing the within-cluster sum of squared distances. The optimal clustering result was obtained according to the minimum intra-cluster dispersion criterion, as described in Equation (1):

$$J = \sum_{i=1}^{k} \sum_{x \in C_i} \|x - \mu_i\|^2 \quad (1)$$

where C_i represents the i-th cluster and μ_i denotes the corresponding cluster centroid. The optimal number of clusters was determined by combining the elbow method and silhouette coefficient analysis. When the number of clusters was set to two, the average silhouette coefficient reached 0.760 on the training set, indicating clear separation between the two fracture modes. The elbow method also showed that intra-cluster dispersion decreased significantly when the cluster number increased from one to two, and the rate of decrease slowed thereafter. Therefore, the two clusters were assigned to tensile and shear fracture modes, respectively. Subsequently, physics-informed labels were constructed based on the clustering results, with tensile fractures assigned a label of 0 and shear fractures assigned a label of 1. This label represents the mesoscopic fracture mechanism state rather than a simple mathematical nonlinear transformation of RA and AF parameters. It introduces explicit mechanical constraints of tensile-shear energy release mechanisms into the subsequent model. To verify the physical validity of the clustering results, the differences in RA, AF, duration, and energy characteristics among different clusters were further statistically analyzed. The proposed physical labels represent the evolution characteristics of fracture mechanisms during the loading process and are introduced into subsequent machine learning prediction models as additional physics-informed prior information.

In conventional AE-based machine learning prediction approaches, models generally rely on statistical features such as amplitude, energy, and frequency to characterize AE responses, while neglecting the influence of fracture mechanisms on the energy release process. To overcome this limitation, this study integrated the RA–AF-based fracture mode identification results with original AE features to construct a physics-informed enhanced feature set. By incorporating fracture mode labels, the model inputs contain not only statistical information of AE signals but also physically meaningful information associated with fracture evolution processes, thereby enabling the transition from traditional data-driven models to physics-informed machine learning models.

2.3. Physics-Informed Feature Optimization and Prediction Framework

AE signals contain abundant information related to material damage evolution; however, different AE feature parameters usually exhibit a certain degree of information redundancy. For example, duration, counts, and energy are all associated with crack activity intensity, whereas frequency-related parameters characterize the dynamic responses during crack propagation. Excessive redundant features not only increase the computational complexity of model training, but may also reduce the capability of prediction models to

identify critical damage-related information. Therefore, effective optimization of input features is required before establishing an AE energy prediction model.

Unlike conventional machine learning approaches that rely solely on statistical AE features, this study incorporated fracture mode information derived from RA–AF analysis to construct physically meaningful input variables. By integrating fracture evolution mechanisms with data-driven modeling, a physics-informed enhanced feature set was developed, which can be expressed as: X_{PI} = [RT, duration, amplitude, counts, PF, CF, RA, AF, FM].

The input features consisted of AE features; RA; AF; and fracture mode label. AE features included rise time, duration, amplitude, counts, peak frequency, and center frequency. The RA and AF parameters characterize the temporal and frequency-related characteristics of fracture propagation, respectively. The fracture mode label (FM label) represents the physics-informed fracture mode information identified from RA and AF features, describing the evolution states of tensile and shear fractures. By incorporating this feature, the model input is no longer limited to the statistical responses of AE signals, but can further capture the influence of fracture mechanisms on the energy release process, thereby enabling the transition from conventional data-driven prediction to physics-informed machine learning.

2.3.1. mRMR-Based Physics-Informed Feature Selection

Input features may exhibit correlations and redundancy among each other; therefore, the minimum redundancy maximum relevance (mRMR) algorithm was employed for feature selection in this study. The mRMR algorithm simultaneously evaluates the relevance between input variables and the target variable, as well as the redundancy among different features, thereby reducing irrelevant information while maintaining predictive capability. For a candidate feature set, the maximum relevance criterion is quantified based on the mutual information between features and the target variable, as expressed in Equation (2), where S represents the selected feature subset and $I(x_i;y)$ represents the mutual information between x_i and y.

$$D = \frac{1}{|S|} \sum_{x_i \in S} I(x_i; y) \tag{2}$$

To reduce information redundancy among features, the mutual information between feature pairs was introduced, as expressed in Equation (3), where $I(x_i;x_j)$ denotes the mutual information between the i-th and j-th input features, with $(i \neq j)$ to exclude self-mutual information terms.

$$R = \frac{1}{|S|(|S|-1)} \sum_{\substack{x_i, x_j \in S \\ i \neq j}} I(x_i; x_j) \tag{3}$$

Finally, the mRMR algorithm achieves optimal feature selection by maximizing the comprehensive objective function that considers both feature relevance and redundancy, as expressed in Equation (4).

$$\max (D-) \tag{4}$$

After mRMR-based feature selection, the top five features retained for model input were, in descending order of importance: duration, fracture mode label, center frequency, amplitude, and peak frequency. Unlike conventional dimensionality reduction methods, mRMR reduces feature redundancy while preserving the inherent physical meaning of variables, which facilitates subsequent analysis of the effects of different fracture-related parameters on prediction performance.

2.3.2. Data Preprocessing and Target Variable Transformation

Because AE energy represents the intensity of local energy release associated with crack propagation, its distribution generally exhibits strong non-uniformity and long-tail characteristics, in which a limited number of intense fracture events account for a dominant proportion of the total energy release. Such highly skewed distributions may cause prediction models to be biased toward extreme values during training, weakening their ability to capture AE energy evolution across different damage stages. Therefore, a base-10 logarithmic transformation was employed to preprocess the AE energy values, as defined in Equation (5), where E denotes the original AE energy and y represents the transformed prediction target. This transformation effectively reduces distribution skewness, alleviates heteroscedasticity, and enhances the model's capability to capture both high-energy fracture events and low-energy AE activities.

$$y = \log_{10}(E + 1) \tag{5}$$

Furthermore, to eliminate the influence of different physical scales on the model training process, the input features were standardized using the Z-score normalization method.

2.3.3. Bayesian Optimization-Based Support Vector Regression Model

After completing the physics-informed feature optimization, an AE energy prediction model based on Bayesian optimization support vector regression (BO-SVR) was further developed. SVR is a machine learning method suitable for small-sample and high-dimensional nonlinear problems. Its fundamental principle is to map input features into a high-dimensional feature space through nonlinear kernel functions and establish the nonlinear relationship between input variables and AE energy based on the structural risk minimization principle. The SVR model performs regression by constructing a regression function, as expressed in Equation (6), where $\varphi(x)$ represents the nonlinear mapping function, and w and b denote the model weight vector and bias term, respectively.

$$f(x) = w^T \phi(x) + b \tag{6}$$

SVR introduces the ε-insensitive loss function to control prediction errors, and its optimization objective can be expressed as Equation (7), where ξ_i and ξ_i^* represent slack variables. C is the penalty parameter that controls the trade-off between model complexity and prediction error.

$$\min \frac{1}{2}\|w\|^2 + C\sum_{i=1}^{n}(\xi_i + \xi_i^*) \tag{7}$$

Since AE energy evolution is jointly governed by fracture modes, damage stages, and multiple physical parameters, the relationship between input variables and energy release exhibits highly complex nonlinear characteristics. Therefore, the radial basis function (RBF) kernel was adopted in this study to establish the nonlinear mapping relationship, as expressed in Equation (8), where γ is the kernel scale parameter that controls the mapping range in the high-dimensional feature space.

$$K(x_i, x_j) = \exp\left(-\gamma\|x_i - x_j\|^2\right) \tag{8}$$

However, the prediction performance of SVR is highly sensitive to its hyperparameters, including the penalty parameter C, kernel parameter γ, and insensitive loss parameter ε. Traditional manual parameter tuning methods suffer from low search efficiency and strong dependence on empirical experience, making it difficult to achieve optimal model performance. Therefore, Bayesian optimization (BO) was employed in this study to auto-

matically optimize the hyperparameters of SVR. Bayesian optimization improves model generalization capability by constructing a surrogate model of the objective function and employing an acquisition function to balance global exploration and local exploitation. The optimization objective is defined as Equation (9), where $\theta = [C, \gamma, \varepsilon]$ represents the hyperparameter combination to be optimized and $f(\theta)$ denotes the cross-validation error of the model. In this study, the expected improvement plus (EI+) strategy was adopted as the acquisition function. The maximum number of objective function evaluations was set to 20. The search ranges of hyperparameters were set as follows: BoxConstraint $\in [10^{-2}, 10^{2}]$, KernelScale $\in [10^{-2}, 10^{2}]$, Epsilon $\in [10^{-4}, 10^{0}]$. By balancing local exploitation around the current optimal solution and exploration of unexplored regions, EI enables efficient searching of the hyperparameter space. Finally, the optimal hyperparameter combination was obtained through Bayesian optimization, and a physics-informed BO-SVR prediction model was established.

$$\theta^{*} = *argmin_{\theta} f(\theta) \tag{9}$$

Unlike conventional data-driven prediction methods, the proposed model incorporates not only statistical features of AE signals but also fracture mode information derived from RA–AF-based fracture identification. This enables the model to learn the nonlinear relationship between fracture evolution mechanisms and energy release behavior.

2.3.4. Model Validation and Evaluation of Physics-Informed Contribution

To validate the prediction reliability of the proposed physics-informed BO-SVR model, this study evaluated its performance from three aspects: model accuracy, generalization capability, and contribution of physics-informed features. All preprocessing steps, including Z-score normalization, K-means clustering, mRMR feature selection, and Bayesian hyperparameter optimization, were performed exclusively on the training dataset. The test dataset was completely held out during the entire training process, and all transformation parameters were derived only from the training set.

Fivefold cross-validation was employed to evaluate the stability of the proposed model. The entire dataset was randomly divided into five mutually exclusive subsets, where four subsets were used for model training and the remaining subset was used for validation. The training and validation processes were repeated five times, and the average coefficient of determination R^2 was calculated according to Equation (10). The standard deviation was calculated using Equation (11) to quantitatively evaluate the prediction stability of the model.

$$\overline{R}^{2} = \frac{1}{k}\sum_{i=1}^{k} R_i^2 \tag{10}$$

$$\sigma_{R^2} = \sqrt{\frac{1}{k-1}\sum_{i=1}^{k} \left(R_i^2 - \overline{R}^{2}\right)^{2}} \tag{11}$$

To verify the effectiveness of the physics-informed enhancement strategy, an ablation experiment based on the fracture mode label was conducted. Under the condition that all other input variables remained unchanged, a complete physics-informed model and a model without fracture mode information were established. By comparing the changes in prediction performance between the two models, the contribution of fracture mode information to AE energy prediction was quantitatively evaluated.

Furthermore, to further interpret the contribution of physics-informed variables during the prediction process, the permutation importance method was introduced to analyze the importance of input features. This method evaluates feature contributions by randomly permuting a specific feature variable and quantifying the decrease in model performance.

To validate the physical interpretability of the fracture mode labels derived from RA–AF clustering, statistical analyses were further conducted to compare the differences in RA, AF, duration, and AE energy characteristics among different clusters. By examining the characteristic responses of AE signals under different fracture modes, the consistency between the automatically identified fracture categories and the actual fracture mechanisms was demonstrated.

Furthermore, per-specimen independent holdout validation was conducted to rigorously evaluate the generalization stability of the method and avoid information leakage of events from the same specimen. Each specimen was independently split into a 70% training set and 30% test set, and all preprocessing steps were performed exclusively on the training set within each specimen. The average performance across all specimens was reported to verify the repeatability of the method across independent samples. The above multidimensional validations demonstrate that the proposed method does not simply introduce an additional data variable, but instead transforms the crack evolution mechanisms reflected by AE signals into physically meaningful prior information that can be recognized by the machine learning model. This enables a transition from conventional data-driven prediction toward physics-informed machine learning.

3. Results and Discussion

3.1. Prediction Performance of the Physics-Informed Machine Learning Framework

To validate the effectiveness of the proposed physics-informed machine learning framework for AE energy prediction of coal gangue backfill, a BO-SVR prediction model was first developed based on the previously constructed physics-informed feature set. The input variables consisted of the key AE features selected by the mRMR algorithm and the fracture mode physical label, while the output variable was the logarithmically transformed AE energy. The model was independently evaluated using the training and testing datasets, and the coefficient of determination (R^2), root mean square error (RMSE), mean absolute error (MAE), and mean squared error (MSE) were adopted as evaluation metrics. Figure 1 presents the comparison between the predicted and measured AE energy values obtained from the BO-SVR model. As shown in the figure, most samples are distributed around the 45° reference line, indicating good agreement between the predicted and experimental values. This demonstrates that the proposed model can effectively capture the complex nonlinear relationship between AE features and energy release behavior. The model achieved an R^2 value of 0.9027, an RMSE of 0.1562, and an MAE of 0.1204 on the testing dataset, indicating that the physics-informed machine learning framework provides highly accurate prediction of AE energy evolution in coal gangue backfill.

To further evaluate the predictive performance of the proposed framework, a comparative analysis was conducted among different machine learning models using the same dataset partition. The compared models included linear regression (LR), support vector regression (SVR), random forest (RF), gradient-boosting decision tree (GBDT), backpropagation neural network (BP), and the proposed BO-SVR model. All models were trained and tested using identical datasets and evaluated with the same performance metrics to ensure the objectivity and consistency of the comparison. The prediction results of different models are presented in Figure 2.

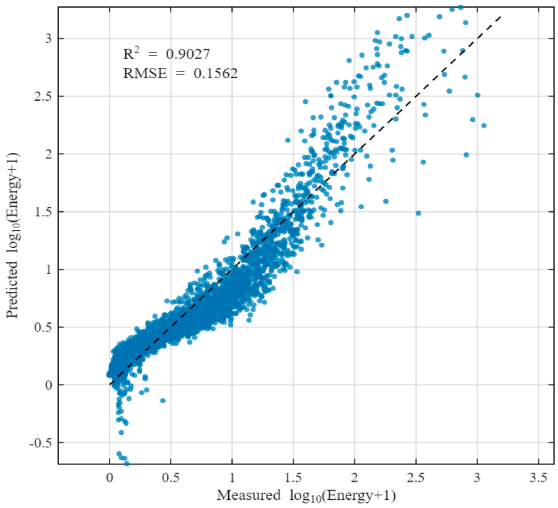


Figure 1. Prediction performance of the BO-SVR model.

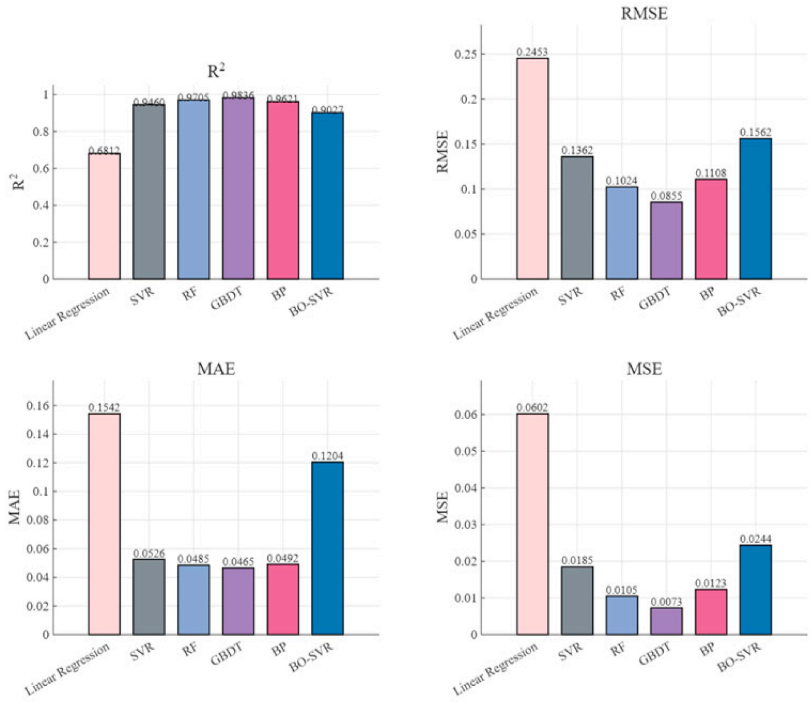


Figure 2. Comparison of performance metrics among different machine learning models.

As shown in Figure 2, all nonlinear machine learning models exhibited significantly better performance than the conventional linear regression model. The linear regression model achieved an R^2 value of only 0.6812, indicating that AE energy release processes exhibit pronounced nonlinear characteristics and cannot be accurately described by simple linear relationships. In contrast, the nonlinear models were capable of effectively learning the complex mapping relationships between AE features and energy evolution. Among these models, the GBDT model achieved the highest prediction accuracy on the independent testing dataset, with an R^2 value of 0.9836. The BP neural network and BO-SVR models also exhibited strong predictive capabilities. These results indicate that under the same training and testing conditions, various nonlinear models are capable of effectively capturing the evolution characteristics of AE energy.

However, the results obtained from a single data partition are insufficient to comprehensively evaluate the generalization capability of the models. Different combinations

of training samples may lead to variations in model performance; therefore, model stability is also an important criterion for evaluating predictive models. To further verify the generalization performance of different models under various data partition conditions, fivefold cross-validation was conducted for systematic evaluation. In addition, an ablation study based on the fracture mode physical label was performed to further investigate the contribution of the physics-informed enhancement strategy to model prediction performance.

It should be noted that the proposed method was initially verified on a single specimen with 4083 valid AE events as a baseline. On the single-specimen dataset, the BO-SVR model achieved an R^2 of 0.9727 and an RMSE of 0.0919 on the test set. When extended to three parallel specimens with a total of 18,992 events, the R^2 decreased to 0.9027 due to increased data dispersion and systematic deviation between specimens. This change is consistent with the characteristics of AE testing: the absolute energy value is highly affected by test system factors such as sensor coupling and specimen contact state, and multi-specimen results are more representative of actual performance in engineering scenarios.

3.2. Generalization Capability of the Model and Contribution Analysis of Fracture Evolution Mechanism Information

Although the independent testing dataset can evaluate the predictive performance of a model, the random division of training and testing datasets introduces certain uncertainty. Therefore, relying solely on a single test result is insufficient to comprehensively assess model generalization capability. In this study, fivefold cross-validation was further employed to systematically evaluate different machine learning models. An ablation study based on the fracture mode physical label was conducted to verify the contribution of the proposed physics-informed enhancement strategy to AE energy prediction performance.

3.2.1. Fivefold Cross-Validation Analysis

To ensure a fair comparison among different models, all models were trained and tested using the same dataset, identical input features, and a consistent cross-validation strategy. The mean coefficient of determination (mean R^2) and standard deviation (STD) obtained from fivefold cross-validation were adopted as evaluation indicators to comprehensively assess both prediction accuracy and model stability. The fivefold cross-validation results of different models are presented in Figure 3.

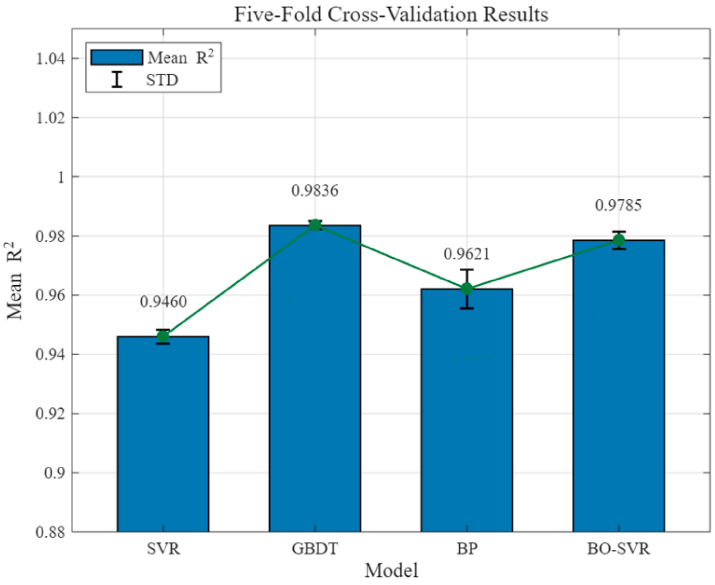


Figure 3. Fivefold cross-validation results of different machine learning models.

As illustrated in Figure 3, all nonlinear models maintained stable performance across different data partitions. The conventional SVR model with default parameters achieved an average R^2 of 0.9460 with a standard deviation of 0.0023, indicating good stability under the same data distribution. The BP neural network achieved an average R^2 of 0.9621 with a standard deviation of 0.0066, showing stable performance on the expanded dataset. The GBDT model exhibited the highest accuracy and stability, achieving a mean R^2 of 0.9836 with a standard deviation of only 0.0014. This indicates that ensemble learning methods can effectively reduce model variance and improve the consistency of prediction results on identically distributed datasets.

It should be noted that ensemble models such as GBDT achieve higher prediction accuracy and stability on identically distributed datasets. However, the core purpose of this study was to investigate the contribution of fracture mode physical information and reveal the underlying mechanism, rather than pursuing the highest prediction accuracy. The BO-SVR model has a clear kernel mapping mechanism and better physical interpretability, which can more clearly quantify the role of physical constraints.

To further verify the stability of the method across independent specimens, per-specimen independent holdout validation was conducted. The proposed BO-SVR model achieved an average R^2 of 0.9044 with a standard deviation of 0.0512 across the three specimens. This result demonstrates that the physics-informed framework maintains reliable performance on different independent specimens, confirming good generalization and repeatability of the method. Therefore, the BO-SVR model was selected as the fundamental model for subsequent physics-informed interpretation analysis in this study.

3.2.2. Contribution Analysis of Fracture Mode Physical Labels

To further verify the independent contribution of the fracture mode label and clarify whether it were merely a nonlinear transformation of RA/AF parameters, four groups of comparative ablation experiments were designed. In all groups, the model structure, training samples, and optimization strategy were kept identical. The four groups were set as follows: (1) model with only RA/AF features; (2) model with only fracture mode label; (3) model with both RA/AF and fracture mode label; (4) full physics-informed model with all conventional AE features and fracture mode label. The results are presented in Figure 4.

The R^2 values of the four groups on the test set were 0.4606, 0.0733, 0.4627, and 0.9027, respectively. Three key conclusions can be drawn: (1) RA/AF parameters have very weak direct correlation with AE energy, and can only explain less than half of the energy variation; (2) the fracture mode label alone has almost no predictive power for absolute energy, confirming that it is not an independent statistical feature; and (3) simply combining RA/AF with the fracture label yields almost no performance improvement compared with RA/AF only, indicating that the label is not a simple nonlinear transformation of RA/AF. (4). Only when the fracture mode label is integrated with all conventional AE features does the performance improve significantly, demonstrating a synergistic enhancement effect.

The results demonstrate that RA and AF have weak direct correlation with AE energy, and the fracture label itself cannot independently predict energy. The significant performance improvement only occurs when the fracture label is integrated with conventional AE features, proving that the label acts as a mechanistic constraint rather than redundant information. It produces a synergistic enhancement effect when combined with conventional statistical features. By incorporating this physical information, the model obtains effective physical constraints for establishing the nonlinear mapping relationship between AE characteristics and energy release behavior.

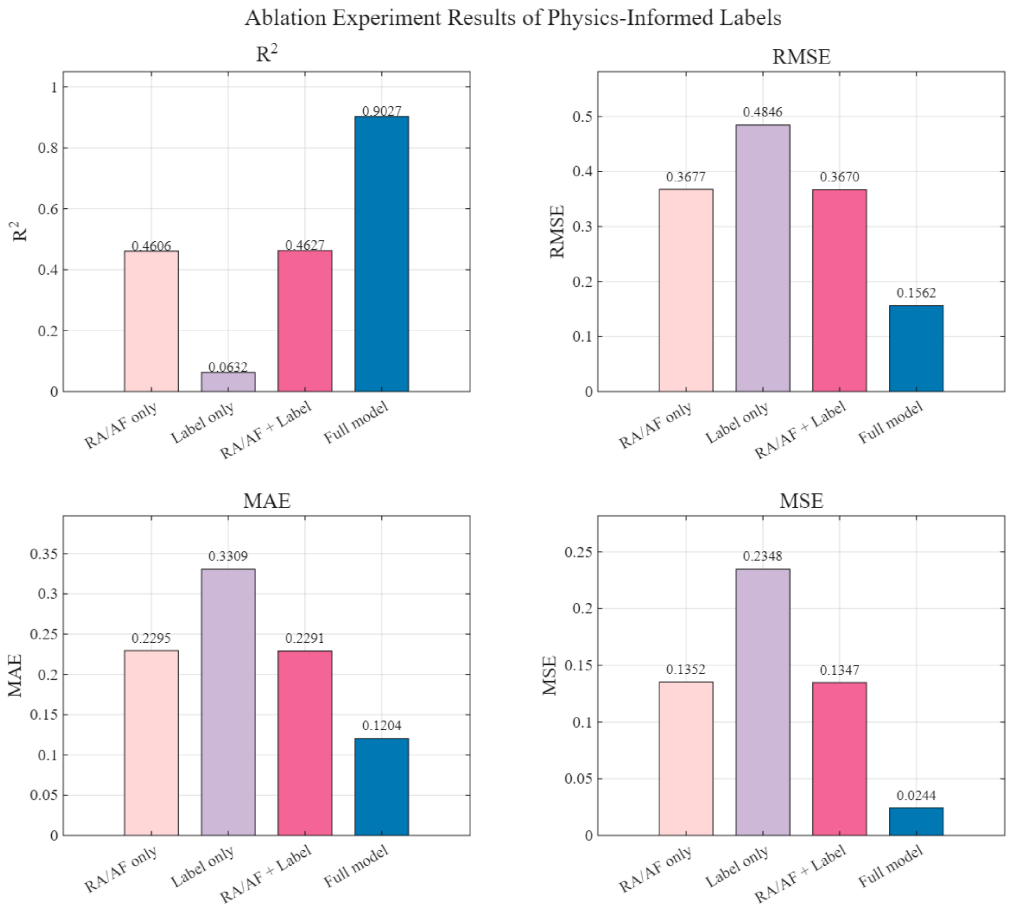


Figure 4. Results of physical information on ablation experiments.

It should be noted that the fracture mode label represents only one component of the physics-informed feature set. Its role is not to replace conventional AE features, but rather to serve as physically meaningful prior information that complements statistical parameters such as duration, amplitude, and frequency to characterize the internal fracture evolution process. Therefore, the improvement in model performance originates from the synergistic integration of statistical information and fracture mechanism information, rather than simply from the increase in the number of input variables.

However, from the perspective of material damage evolution, the improvement brought by the fracture mode label does not originate from simply adding an additional input variable, but rather from the crack propagation mechanism information embedded in AE signals. During the compression process of coal gangue-filled backfill, the initiation, propagation, and coalescence of microcracks are accompanied by distinct energy release behaviors. Tensile cracks are mainly characterized by rapid crack opening and instantaneous energy release, whereas shear cracks generally involve frictional sliding along crack surfaces, resulting in a more prolonged failure process and higher energy dissipation.

Conventional AE features, such as amplitude, duration, counts, and frequency, primarily describe the external response characteristics of AE signals, but cannot directly distinguish different fracture mechanisms. By identifying fracture modes in the RA–AF parameter space and converting them into physics-informed labels, the proposed model is able to further capture the influence of fracture types on energy release processes. This enables a transition from conventional "signal feature learning" toward "fracture mechanism-aware prediction."

3.3. Physical Interpretation of Fracture Mode Information

To further elucidate the underlying reasons for the improved performance of the physics-informed machine learning framework, the contribution of fracture mode physical labels was analyzed from two perspectives: model feature importance and fracture mode evolution mechanisms. First, permutation importance was employed to quantify the contribution of different input variables to model prediction. Subsequently, the physical characteristics associated with different fracture modes were investigated based on the RA–AF clustering results, providing insights into the intrinsic mechanism by which fracture mode information enhances prediction performance.

3.3.1. Contribution Analysis of Input Features

To quantitatively evaluate the importance of different input variables to model predictions, the permutation importance method was employed for feature contribution analysis. This method evaluates feature importance by randomly permuting one input variable and measuring the corresponding change in model prediction error. A larger performance degradation after perturbing a specific variable indicates a greater contribution of that variable to the prediction results. The importance ranking of all input variables is presented in Figure 5.

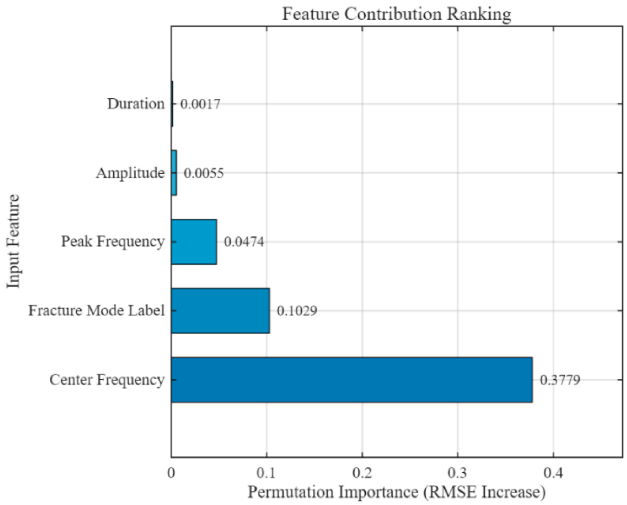


Figure 5. Contribution of input features based on permutation importance analysis.

Duration exhibited the highest contribution among all input variables, with an importance value of 0.3779. This result indicates that AE duration effectively reflects the persistence of energy release during crack propagation and serves as the most influential statistical parameter for AE energy prediction.

Amplitude and peak frequency exhibited importance values of 0.1029 and 0.0474, respectively. These parameters characterize the transient response intensity and frequency-domain characteristics during crack propagation, respectively, and collectively determine the statistical characteristics of AE signals.

The fracture mode label exhibited an importance value of 0.0055, and center frequency exhibited the lowest importance of 0.0017. Although the permutation importance of the fracture mode label was relatively low in the full feature set, ablation experiments confirmed that it provided unique mechanistic constraints that could not be replaced by individual statistical features. Its value lies in guiding the model to establish mapping relationships consistent with fracture physics, rather than directly contributing to variance explanation.

3.3.2. Energy Dissipation Characteristics of Different Fracture Modes

To further validate the physical significance of the fracture mode label, statistical analyses were performed on different fracture modes identified by RA–AF clustering. The corresponding RA, AF, average AE energy, and duration characteristics of each cluster are summarized in Table 1.

Table 1. RA, AF, average AE energy, and duration characteristics of different fracture mode clusters.

Cluster	Mean RA	Mean AF	Mean Energy	Mean Duration
Cluster 1	0.8754	0.0964	13.119	465.67
Cluster 2	0.0124	1.0535	0.0178	1.326

Based on the RA–AF clustering analysis, Cluster 1 and Cluster 2 exhibited distinct differences in mesoscopic fracture behavior and energy release characteristics. Cluster 1 was characterized by high RA, low AF, long duration, and high energy, corresponding to shear fracture dominated by interfacial frictional sliding. Cluster 2 featured low RA, high AF, short duration, and low energy, consistent with tensile fracture dominated by instantaneous crack opening. These characteristic patterns are highly consistent with the classical RA–AF tensile-shear fracture criterion—a well-established methodology in the acoustic emission community that has been extensively validated by independent studies combining source location, digital image correlation (DIC), and high-speed imaging. This consistent correspondence provides strong indirect validation for the physical significance of the clustering labels.

The shear fracture cluster (Cluster 1) showed higher RA values and lower AF values, with average RA and AF values of 0.8754 and 0.0964, respectively. It exhibited longer duration (465.67 μs) and higher average AE energy (13.119). This set of characteristics corresponds to the typical features of shear fracture: frictional sliding along crack surfaces leads to a sustained fracture process and continuous energy dissipation.

In contrast, the tensile fracture cluster (Cluster 2) exhibited lower RA values and higher AF values, with average RA and AF values of 0.0124 and 1.0535, respectively. Its duration was only 1.326 μs, and the average AE energy was 0.0178. This matches the characteristics of tensile fracture: rapid crack opening results in instantaneous energy release with a short rise time and high oscillation frequency.

Quantitative analysis revealed that the average AE energy released by shear fractures was approximately 739 times that of tensile fractures. The huge difference in energy release intensity further confirms that the two clusters correspond to fundamentally different fracture mechanisms, rather than arbitrary mathematical partitions. Although tensile fractures represent the primary form of early-stage damage initiation, the energy dissipation associated with individual tensile fracture events is relatively limited. In contrast, shear failure involves complex energy dissipation mechanisms, including interfacial frictional sliding, particle interlocking and shearing, and structural rearrangement, which are the primary factors controlling the development of macroscopic shear fractures and high-energy AE release.

The above results demonstrate that the fracture modes identified by RA–AF clustering are not artificially constructed discrete labels, but rather physical state variables capable of reflecting different crack propagation mechanisms and energy release characteristics. Therefore, by introducing the fracture mode label into the machine learning model, the prediction framework gains prior knowledge of fracture evolution pathways, allowing the prediction process to rely not only on statistical patterns of AE signals but also on constraints imposed by fracture mechanisms.

3.4. Controlling Mechanisms of Fracture Mode Evolution and AE Energy Release

3.4.1. Mesoscopic Damage and Fracture Network Evolution Mechanisms in Coal Gangue-Filled Backfill

During uniaxial loading, AE energy release is essentially governed by the initiation, propagation, and topological interaction of microcracks, rather than simply reflecting macroscopic statistical damage evolution. As illustrated in Figure 6, coal gangue-filled backfill is a typical heterogeneous granular material containing abundant pores and weakly bonded regions, such as matrix–aggregate interfaces. Therefore, its failure process is not dominated by a single cracking mode, but instead exhibits a progressive evolution involving five distinct stages.

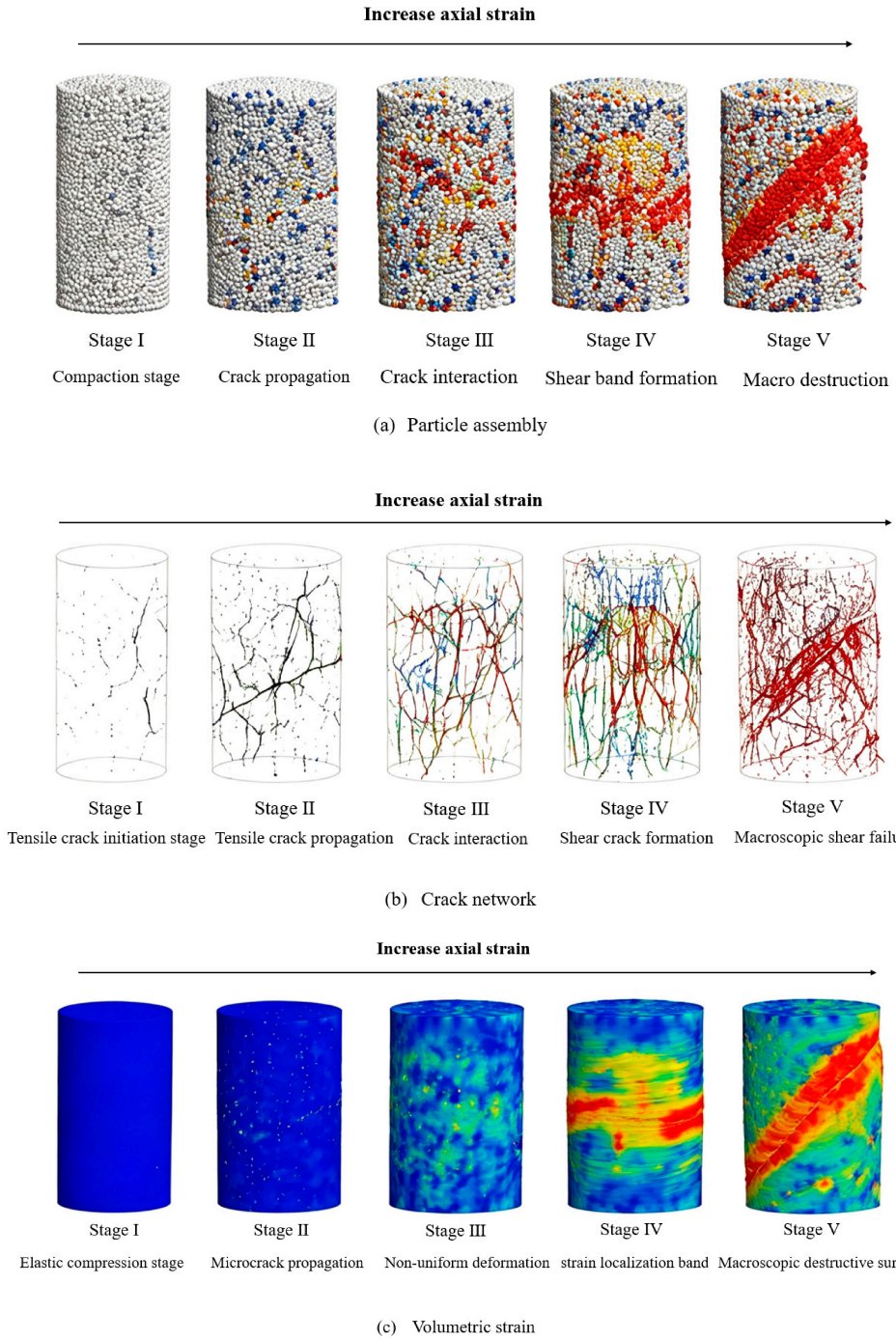


Figure 6. Progressive failure and crack evolution process of coal gangue-filled backfill under uniaxial compression.

During the compaction and microcrack initiation stage, the external load is primarily consumed in closing initial pores and overcoming weak bonding defects, as shown in Figure 6a. According to Figure 6b, the mesoscopic damage at this stage is dominated by localized tensile cracking, where crack propagation is mainly controlled by stress concentration around pore edges, with no significant shear damage observed. With increasing strain accumulation, micro-tensile cracks gradually propagate and begin to interact with each other. The high shear stress concentration at crack tips induces relative sliding between particles, causing the fracture evolution to gradually transition from tensile-dominated cracking to a mixed tensile–shear failure mode. As shown in Figure 6c, this transition process is accompanied by the development of localized strain zones. When the critical peak strength is reached, discrete cracks coalesce into continuous macroscopic shear bands, corresponding to Stages IV–V in Figure 6a,b. At this stage, intense interparticle frictional sliding, particle rearrangement, and sustained slip along the dominant shear plane generate significant strain localization, ultimately leading to structural instability of the backfill and triggering high-intensity AE energy release.

3.4.2. Interpretation of AE Energy Evolution Based on Fracture Mode Constraints

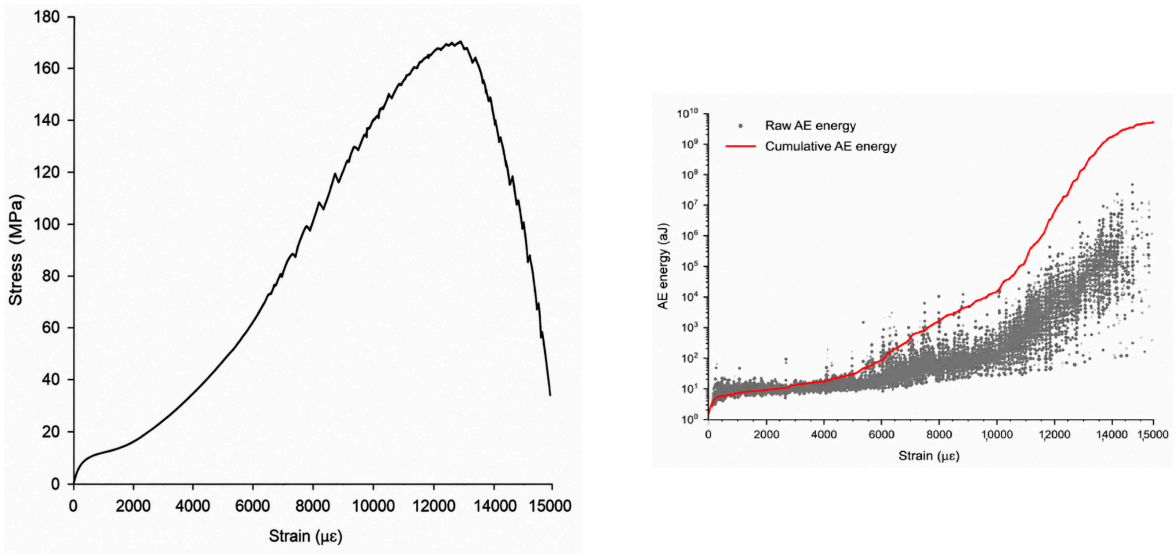
To further reveal the mechanism by which fracture mode information contributes to AE energy prediction, the model prediction results were correlated with the damage evolution stages during the loading process of coal gangue-filled backfill. By integrating the stress–strain response, AE energy evolution, tensile–shear fracture ratio variation, and the evolution of model prediction errors, a fracture mode-constrained framework for interpreting AE energy release mechanisms was established, as illustrated in Figure 7.

During the initial compaction stage, the applied load is primarily consumed by closing preexisting pores and eliminating loose contacts between particles within the specimen, resulting in rapid compaction deformation. At this stage, AE events are relatively limited, and the cumulative AE energy remains at a low level. The fracture activity is mainly associated with the closure of existing defects and local adjustment of weak interfaces. Since no significant newly generated cracks have developed, the RA–AF analysis indicates that this stage is dominated by low-energy tensile microcrack events. As AE signals mainly originate from local structural adjustments, the variation range of statistical parameters is relatively limited. Consequently, model prediction at this stage relies mainly on basic AE parameters such as duration and counts, while the contribution of fracture mode information remains relatively low.

With further loading, the specimen enters the elastic deformation stage, during which particle contacts gradually become stabilized and new microcracks begin to initiate and propagate slowly. During this stage, AE energy exhibits a gradual increasing trend, accompanied by an increase in the number of fracture events, while the overall fracture development remains constrained by the surrounding particle structure. In terms of fracture mode evolution, tensile cracks still dominate during this stage. This is mainly attributed to the fact that tensile stress acting on the bonding regions between coal gangue particles initially induces interface debonding and tensile opening failure. Since tensile cracks are primarily associated with the formation of new fracture surfaces, the corresponding energy release is relatively limited, resulting in a relatively small increase in AE energy.

After entering the stable crack propagation stage, microcracks gradually extend and undergo local coalescence with continuous loading, resulting in a significant increase in AE activity. During this stage, AE energy begins to increase rapidly, while the RA–AF clustering results indicate that the fracture mode gradually evolves from a single tensile-dominated mechanism toward a mixed tensile–shear mode. Since different fracture mechanisms may generate AE signals with similar statistical characteristics, relying solely on conventional

parameters such as amplitude and duration may lead to confusion between fracture events governed by different mechanisms. By introducing the fracture mode label, the model is able to distinguish AE events according to their underlying fracture mechanisms, thereby improving its capability to characterize the AE energy evolution process.



(**a**) Stress-strain curve

(**b**) AE energy evolution

(**c**) Tensile/Shear ratio evolution

(**d**) Prediction error evolution ($\log_{10}$(E+1))

Figure 7. AE energy release mechanism under fracture mode constraints.

When the applied load approaches the peak strength, internal cracks rapidly propagate and coalesce, leading to the unstable damage stage. During this stage, AE energy increases dramatically and reaches the dominant energy release phase. The proportion of shear fractures increases significantly. By incorporating fracture mode constraints, the physics-informed model is able to distinguish the differences in energy release associated with different fracture mechanisms, thereby maintaining relatively low prediction errors even during rapid damage evolution.

After reaching the peak strength, through-going macroscopic cracks are formed within the specimen, resulting in rapid instability of the load-bearing structure. During this stage, AE energy reaches its maximum value and subsequently decreases due to the reduction of effective load-bearing regions, leading to a gradual attenuation of AE activity. The fracture mode exhibits highly concentrated shear-dominated characteristics, indicating that the final failure is primarily controlled by crack coalescence and particle sliding. The model prediction results demonstrate that during the macroscopic failure stage, the fracture mode

information provides sufficient characterization of the changes in fracture mechanisms, enabling the physics-informed model to more accurately capture abrupt variations in AE energy.

3.4.3. Underlying Mechanism of Prediction Performance Improvement by Introducing Physical Labels

Traditional AE statistical features can only characterize the macroscopic external responses of acoustic emission signals, but are insufficient to distinguish the underlying mesoscopic fracture mechanisms. For example, two AE events with similar amplitudes may originate from fundamentally different damage processes, such as low-energy and rapid-release microscopic tensile cracking or high-energy and prolonged macroscopic shear sliding. These two fracture mechanisms exhibit essential differences in their energy release behaviors.

The introduction of fracture mode labels effectively imposes explicit mechanical constraints on the machine learning framework. Such labels do not simply increase the dimensionality of input features: instead, they constrain the optimization space of the algorithm within a physically meaningful domain consistent with actual fracture evolution and damage mechanisms. Consequently, the model establishes a more physically realistic mapping between AE parameters and internal damage energy release, thereby significantly improving the prediction accuracy and generalization capability of AE energy estimation.

It should be noted that RA–AF values and the derived fracture mode classification are sensitive to acquisition conditions, including sensor type, resonant frequency, sampling rate, and amplitude threshold. In this study, all AE signals were recorded using identical RS-2A sensors, consistent acquisition settings (3 MHz sampling rate, 40 dB preamplifier gain, 45 dB detection threshold), and a standardized coupling procedure to ensure reliable and consistent RA–AF calculation across specimens. Independent validation combining DIC and high-speed imaging will be conducted in follow-up work to directly visualize the mesoscopic fracture process and corroborate fracture mode assignment.

4. Conclusions

Aiming at the demand for accurate AE energy estimation and physical mechanism interpretation in coal gangue backfill damage monitoring, this paper proposes a fracture mode-constrained physics-informed machine learning framework. Based on 18,992 valid AE events from three parallel specimens with identical mix proportion and curing conditions, the BO-SVR model achieved an R^2 of 0.9027 and an RMSE of 0.1562 under the 7:3 random holdout test. The per-specimen independent holdout validation further yielded an average R^2 of 0.9044 with a standard deviation of 0.0512, confirming the stable repeatability of the method across independent specimens. It should be noted that the method was initially verified on a single specimen with 4083 events, achieving an R^2 of 0.9727 under the same distribution. The slight decrease in R^2 in the multi-specimen dataset is attributed to increased data dispersion and systematic deviation between specimens, which is more representative of actual performance in engineering scenarios.

Four-group ablation experiments demonstrated that the fracture mode label is not a simple nonlinear transformation of RA/AF parameters. The RA/AF features alone only explain less than half of the energy variation, and the label alone has almost no independent predictive power. Only when the fracture mode label is integrated with conventional AE statistical features does the performance improve significantly, showing a clear synergistic enhancement effect. This indicates that the fracture mode label acts as a mechanistic constraint rather than an independent statistical feature, which guides the model to establish a mapping relationship consistent with tensile-shear fracture physics.

Permutation importance analysis further confirmed that duration was the most influential statistical feature for energy prediction, which is consistent with the physical nature of AE energy as a time-integrated quantity, while the fracture mode label exerted its value at the mechanism level.

Mesoscopic mechanism analysis revealed that the two clusters identified by RA–AF clustering corresponded to fundamentally different fracture modes. The average energy released by shear fracture was approximately 739 times that of tensile fracture. Tensile fracture dominated the early compaction and crack initiation stage with instantaneous energy release, while shear fracture dominated the later crack coalescence and macroscopic failure stage with sustained frictional energy dissipation. The transition from tensile-dominated to shear-dominated energy release revealed the progressive damage evolution law of cemented gangue backfill under uniaxial compression.

This study still has certain limitations. RA–AF values and the corresponding fracture mode identification are affected by sensor type, sampling frequency, and amplitude threshold settings. In addition, the current research was based on laboratory uniaxial compression tests, and the absolute energy prediction across different test systems still has constraints. In future work, independent verification of fracture modes will be carried out, combined with digital image correlation technology, and the proposed framework will be extended to more complex stress paths such as triaxial compression and cyclic loading, to further improve its engineering applicability in field backfill stability monitoring.

Author Contributions: J.L.: conceptualization, methodology, administration, writing—original draft. P.W.: conceptualization, formal analysis, project administration. J.J.: data curation. B.L.: investigation, validation. Z.L.: resources, formal analysis. S.Z.: visualization. All authors have read and agreed to the published version of the manuscript.

Funding: This research was funded by the Liaoning Provincial Natural Science Foundation under grant [024-BS-259], the Basic Scientific Research Project of the Department of Education of Liaoning Province under grant [LJ212410147017] and the National Natural Science Foundation of China under grant [52404125].

Institutional Review Board Statement: Not applicable.

Informed Consent Statement: Not applicable.

Data Availability Statement: The data will be made available upon request.

Acknowledgments: This work was supported by the Doctoral Start-Up Project of the Liaoning Provincial Natural Science Foundation under grant 2024-BS-259, the Basic Scientific Research Project of the Department of Education of Liaoning Province under grant LJ212410147017, and the National Natural Science Foundation of China under grant 52404125.

Conflicts of Interest: The authors declare no conflicts of interest.

References

1. Wang, H.; Feng, G.; Qi, T.; Wang, L.; Ding, Q.; Pan, D.; He, J. Insight into the fracture mechanical properties of the interfacial transition zone of cemented coal gangue backfill under different stress angles by mesoscopic digital image correlation. *Eng. Fract. Mech.* **2024**, *300*, 109988. [CrossRef]
2. Guo, S.; Zhang, H.; Yuan, C.; Bi, Y. Alkali-activated steel slag-coal gangue cementitious materials: Strength, hydration, and heavy metal immobilization. *Case Stud. Constr. Mater.* **2025**, *23*, e05120. [CrossRef]
3. Kong, X.; Yang, J.; Mao, D. Research progress on green mining technology of coal under the background of "dual carbon". *Mod. Coal Mines* **2026**, *online first*. Available online: https://link.cnki.net/urlid/37.1205.TD.20260413.1023.002 (accessed on 1 September 2026).
4. Wu, F.; Bai, J.; Feng, G.; Han, Y. Investigation on mechanical properties and micro-mechanisms of low-carbon cemented paste backfill utilizing steel-slag binder. *Powder Technol.* **2026**, *480*, 122673. [CrossRef]

5. Zhao, G.; Zhang, Y.; Zhang, G.; Zhang, H.; Zhang, X. Effects of mass concentration and curing age on the mechanical properties and damage evolution of aeolian sand backfill. *Sci. Rep.* **2026**, *16*, 6321. [CrossRef] [PubMed]
6. Li, L.; Zhang, M.; Li, Y.; Duan, Z.B. Hydro-mechanical coupling elastoplastic constitutive model of unsaturated loess considering structural evolution. *Rock Soil Mech.* **2026**, *47*, 2665–2675. [CrossRef]
7. Lubliner, J.; Oliver, J.; Oller, S.; Oñate, E. A plastic-damage model for concrete. *Int. J. Solids Struct.* **1989**, *25*, 299–326. [CrossRef]
8. Feng, G.; Kang, Y.; Sun, Z.; Wang, X.; Hu, Y. Effects of supercritical CO_2 adsorption on the mechanical characteristics and failure mechanisms of shale. *Energy* **2019**, *173*, 870–882. [CrossRef]
9. Shi, Z.; Zhang, Y. Prdiction of freeze-thaw resistance of geopolymer mortar based on Weibull distribution model. *J. Inn. Mong. Agric. Univ. (Nat. Sci. Ed.)* **2026**, *online first*. Available online: https://link.cnki.net/urlid/15.1209.s.20260509.1018.008 (accessed on 1 September 2026).
10. Deng, W.; Chai, J.; Yang, J.; Yang, Z.; Yin, X.; Tian, G.; Gao, C. InSAR prediction of surface uplift in closed coal mining areas using a combination of Weibull function and Kalman filtering. *J. Min. Rock Control Eng.* **2025**, *7*, 207–218. [CrossRef]
11. Deng, L.; Yuan, H.; Su, G.; Chen, J.; Chen, Y.; Zhang, M. Shear-induced acoustic emission and energy evolution in granular-filled active waveguide. *Results Eng.* **2025**, *26*, 105079. [CrossRef]
12. Wei, C.; Chan, C.M.; Wu, W.; Su, X.; Gu, Y.; Liu, M. Experimental investigation and discrete element modeling of acoustic emission characteristics, crack evolution, and energy variation in shale specimens during uniaxial compression. *Results Eng.* **2025**, *28*, 108317. [CrossRef]
13. Wu, Y.; Li, X.; Kong, L.; Luan, H.; Liu, X.; Liu, Z.; Liu, B. Study on the mechanical properties and failure evolution of multi-fractured rock based on AE and DIC techniques. *China Min. Mag.* **2026**, *35*, 99–109. [CrossRef]
14. Tian, Y.; Sun, H.; Wang, Y.; Yan, L.Y. Mechanisms of stress memory formation and decay in granite via multi-parameter acoustic emission. *Measurement* **2026**, *279*, 121841. [CrossRef]
15. Yuan, B.; Choo, C.S.; Yeo, L.Y.; Wang, Y.; Yang, Z.; Guan, Q.; Suryasentana, S.; Choo, J.; Shen, H.; Megia, M.; et al. Physics informed machine learning in geotechnical engineering: A direction paper. *Geomech. Geoengin.* **2025**, *20*, 1128–1159. [CrossRef]
16. Zhou, W.; Yang, C.; Wang, S.N.; Shen, Y.-N.; Wang, Y.-B.; Sun, H. Size effect and damage evolution of CFRP tubes under radial compression using acoustic emission and deep learning. *Appl. Compos. Mater.* **2026**, *33*, 136. [CrossRef]
17. Kwon, J.H.; Lee, H.W.; Cho, S.; Lee, D.; Jo, A.R.; Hwang, S.-K.; Chae, H.; Woo, W.; Kim, D.-K. Data-driven acoustic emission framework with multimodal validation for resolving micromechanical damage in B4C/AA6061 composite. *Compos. Part B Eng.* **2026**, *325*, 114010. [CrossRef]
18. Karahan, H.; Alkaya, D. Ensemble machine learning for predicting TBM penetration rate with limited geotechnical data. *Appl. Sci.* **2026**, *16*, 3451. [CrossRef]
19. Memiş, M.A.; Keskin, I.; Demir, S.; Memiş, Ş.U. Machine learning-based prediction of permafrost degradation and its implications on geotechnical infrastructure: A comprehensive review. *AI Civ. Eng.* **2025**, *4*, 28. [CrossRef]
20. Yang, R. The application of big data technology in geological and geotechnical engineering investigation. *Intell. Build. Smart Cities* **2025**, 38–40. [CrossRef]
21. Zhang, W.; Li, H.; Li, Y.; Liu, H.; Chen, Y.; Ding, X. Application of deep learning algorithms in geotechnical engineering: A short critical review. *Artif. Intell. Rev.* **2021**, *54*, 5633–5673. [CrossRef]
22. Eshraghi, A.; Kodjo, S.A.; Rivard, P.; Shams, G. Machine-learning-based crack mode classification in plain concrete considering acoustic emission wave propagation effects. *Constr. Build. Mater.* **2025**, *489*, 142188. [CrossRef]
23. Lü, L.; Li, X.; Yang, Y.; Wan, Y.; Fu, Y. Comparative study on predicting the consolidation yield stress of geotechnical materials using different machine learning methods. *J. Taiyuan Univ. Technol.* **2026**, *online first*. Available online: https://link.cnki.net/urlid/14.1220.N.20260430.1405.006 (accessed on 1 September 2026).
24. Lu, D.; Fu, K.; Sun, Z.; Dai, J.; Gao, C.; Hou, Q. Inversion of mechanical parameters and dynamic response analysis of dangerous rock mass slopes after earthquakes. *Min. Metall. Eng.* **2025**, *45*, 34–40. [CrossRef]
25. Karniadakis, G.E.; Kevrekidis, I.G.; Lu, L.; Perdikaris, P.; Wang, S.; Yang, L. Physics-informed machine learning. *Nat. Rev. Phys.* **2021**, *3*, 422–440. [CrossRef]
26. Peng, H.; Long, F.; Ding, C. Feature selection based on mutual information criteria of max-dependency, max-relevance, and min-redundancy. *IEEE Trans. Pattern Anal. Mach. Intell.* **2005**, *27*, 1226–1238. [CrossRef] [PubMed]
27. Meysami, M.; Lotfi, A.; Salehi, S. Deep learning and the geometry of compactness in stability and generalization. *Mach. Learn. Appl.* **2026**, *23*, 100820. [CrossRef]
28. Jin, J.; Liu, T.; Li, M.; Lv, T.; Zhang, S.; Zuo, S. Mechanical properties and compression damage characteristics of coal gangue-filled backfill cemented by fly ash modified self-consolidating grouts. *Case Stud. Constr. Mater.* **2025**, *22*, e04687. [CrossRef]
29. Jin, J.; Gu, X.; Li, M.; Qin, Z.; Liu, T.; Wu, P.; Zuo, S. Effect of aggregate surface strengthening on compressive damage of pre-placed coal gangue cemented backfill. *Coal Sci. Technol.* **2025**, *53*, 277–291. [CrossRef]
30. Shen, F.; He, S.; Song, D.; He, X.; Yang, G.; Baig, O. Response characteristics of acoustic emission signal and judgment criteria for different fracture modes. *Eng. Fract. Mech.* **2024**, *296*, 109862. [CrossRef]

31. Chang, X.; Wu, S.; Cheng, H.; Fu, X. Full-waveform characteristics and frequency spectrum of acoustic emission for fine sandstone. *J. Yangtze River Sci. Res. Inst.* **2022**, *39*, 118–125. [CrossRef]
32. Mathias, S.G.; Akmal, M.U.; Asif, S.; Koval, L.; Knollmeyer, S.; Grossmann, D. Pattern identifications in transformed acoustic signals using classification models. *Procedia CIRP* **2024**, *130*, 93–99. [CrossRef]
33. Li, X.; Chen, D.; Liu, S.; Chen, S.; Feng, F.; Li, Z.; Wang, E.; Zhai, M. Multi-scale correlation analysis of acoustic emission characteristics and energy evolution process of cavernous fractured sandstone. *J. Min. Rock Control Eng.* **2025**, *7*, 043011. [CrossRef]
34. Aggelis, D.G. Classification of cracking mode in concrete by acoustic emission parameters. *Mech. Res. Commun.* **2011**, *38*, 153–157. [CrossRef]
35. Du, K.; Luo, X.; Liu, M.; Liu, X.; Zhou, J. Understanding the evolution mechanism and classification criteria of tensile-shear cracks in rock failure process from acoustic emission (AE) characteristics. *Eng. Fract. Mech.* **2024**, *296*, 109864. [CrossRef]

Disclaimer/Publisher's Note: The statements, opinions and data contained in all publications are solely those of the individual author(s) and contributor(s) and not of MDPI and/or the editor(s). MDPI and/or the editor(s) disclaim responsibility for any injury to people or property resulting from any ideas, methods, instructions or products referred to in the content.